Seven-core photonic liquid crystal fibers for simultaneous mode shaping and temperature sensing

Min Liu (刘 敏)[1,2,*], Bingyue Zhao (赵昺玥)[1,2], Xu Yang (杨 虚)[1,2], and Jingyun Hou (侯静云)[1,2]

[1]*College of Communication Engineering, Chongqing University, Chongqing 400044, China*
[2]*Key Laboratory of Optoelectronic Technology and Systems (Education Ministry of China), Chongqing University, Chongqing 400044, China*
**Corresponding author: liumin@cqu.edu.cn*

Received December 14, 2016; accepted March 9, 2017; posted online March 23, 2017

Through doping liquid crystals into the core region, we propose a kind of seven-core photonic crystal fiber (PCF) which can achieve mode shaping and temperature sensing simultaneously in the communication window of 1.1–1.7 μm. To the best of our knowledge, this is the first time that the function of seven-core PCFs as temperature sensors is investigated. By using the full vectorial finite element method, the characteristics of the fiber with the temperature, such as the effective mode area, the waveguide dispersion, and the confinement loss, are analyzed. This kind of PCF can be competitive in providing temperature sensing in multi-core PCF lasers.

OCIS codes: 050.5298, 160.3710, 060.5295.
doi: 10.3788/COL201715.060601.

The photonic crystal fiber (PCF), which is infiltrated with special materials, has the advantage of effectively combing the holey micro structure with the physical properties of the materials[1]. This kind of combination can provide the PCF with various responses, corresponding to different external fields. The infiltrated PCFs can find many applications, such as optical mode converters[2], fiber beam splitters[3], optical fiber sensors[4,5], fiber lasers[6], etc.

The liquid crystal (LC) is a special kind of material whose index is related to the temperature and the electric field intensity[7,8]. The LC has been widely used in many kinds of photonic devices, such as projection displays, tunable photonics[9–11], and depolarizers[12]. Through infiltrating the PCF with LCs, the PCF exhibits novel propagation characteristics, which makes it applicable to temperature sensing, the polarization splitter, the variable attenuator, etc. Sun *et al.* have demonstrated the broadband thermo-optic switching effect based on LC-filled PCFs[13]. A highly tuned large-core single-mode LC photonic bandgap fiber has been proposed, which has a large temperature gradient of the refractive indices at room temperature[14]. A novel polarization splitter based on dual-core PCFs with an LC modulation core was investigated[15]. The dispersion properties of LC core PCFs was studied by Karasawa, which can be utilized for various applications including the spectral control of supercontinuum generation[16,17]. Mathews *et al.* have experimentally demonstrated an all-fiber variable optical attenuator based on the LC infiltrated PCF[18]. Milenko *et al.* have proposed a temperature-sensitive photonic LC fiber modal interferometer[19]. A fiber Sagnac interferometer based on a liquid-filled PCF for temperature sensing was proposed in Ref. [20].

In this Letter, we design a new kind of seven-core PCF infiltrated with E7 LC, which has an ultralow confinement loss. By using the full vectorial finite element method, the properties of the PCF caused by the infiltration are investigated. We find that the mode intensity of the infiltrated cores, the effective mode area, the waveguide dispersion, and the confinement loss are dependent on the temperature. The most important feature of the fiber is that the mode shaping and temperature sensing can be realized simultaneously without varying the structure. This kind of novel multi-core PCF can be used in optical fiber temperature sensors or splitters, which are sensitive to the temperature.

The structure of the proposed PCF is shown in Fig. 1. The red part of the structure is the cores, which are infiltrated with an E7 LC with an ultralow confinement loss. The diameter of the infiltrated cores "D" is 2.2 μm. The diameter of all air holes "d" is 1.2 μm. The hole to hole distance is Λ. For ensuring that the light is transmitted in the single-mode condition, d/Λ is set to be 0.45. The air holes nearest to the center core have significant influence on the infiltrated cores, and the diameter of them is labeled as a. The temperature is set to be 25°C, and the operating wavelength is 1.55 μm.

The index of LCs is related to the temperature and the wavelength, which can be described as the Cauchy equation:

$$n_o = A_o + B_o/\lambda^2 + C_0/\lambda^4, \tag{1}$$

$$n_e = A_e + B_e/\lambda^2 + C_e/\lambda^4, \tag{2}$$

where n_o and n_e represent the ordinary and extraordinary refractive index, and the Cauchy coefficients A_i, B_i, C_i $(i = o, e)$ are related to the temperature, which can be obtained through the experiments[21].

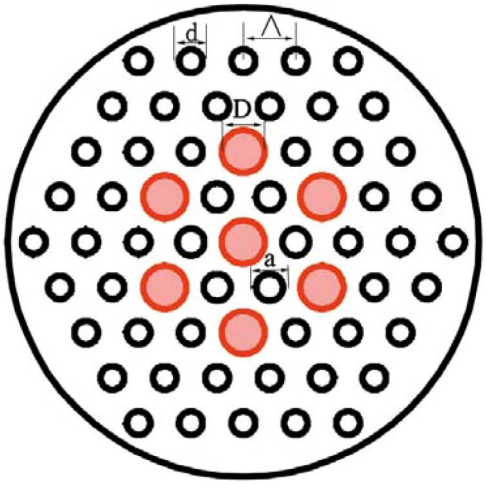

Fig. 1. Structure of the designed PCF.

Mode shaping is a feasible way to effectively improve the output power of the coherent beam combination of PCFs, and it can also optimize the beam quality of PCFs. In order to achieve mode shaping, we need to observe the mode intensity of each infiltrated core. Due to the symmetry of the structure, only the intensity distribution of the infiltrated cores along the y axis is shown in Fig. 2 with diameter "a" varying from 1.2 to 1.4 μm. It can be seen that when diameter "a" decreases, the intensity of the center core decreases, whereas the intensity of the surrounding cores increases. This is mainly because when diameter "a" decreases, the mode field area increases, which makes the energy of the center core easily coupled to the surrounding cores. It implies that optimizing diameter "a" makes it possible to realize a roughly identical intensity of each core, i.e., mode shaping. Through trials, we find that the mode shaping of the infiltrated seven-core PCF can be obtained when $a = 1.37$ μm.

Based on the mode-shaping infiltrated PCF, we study the effects of the temperature on the mode field distribution, as shown in Fig. 3, with $D = 2.2$ μm, $d = 1.2$ μm, $a = 1.37$ μm, and $d/\Lambda = 0.45$. The temperature changes from 15°C to 35°C, which is a reasonable operating range considering that the fibers require water-cooling in high power working conditions. It can be intuitively seen that in the mode-shaping PCF, the intensity of each infiltrated core is nearly the same for different temperatures. When the temperature increases from 15°C to 35°C, the mode field intensity in the cores decreases. In order to show the effects of the temperature on the mode intensity clearly, Fig. 4 is given with the same parameters of Fig. 3. It can be explicitly observed that when the temperature increases from 15°C to 35°C, the intensity decreases from 8.926×10^{16} to 8.031×10^{16} W/m^2.

The relationship between the peak value of the mode intensity and the temperature at different diameter "D", which ranges from 2 to 2.5 μm is shown in Fig. 5. It is indicated that for any value of diameter "D", the peak mode intensity is inversely proportional to the temperature, which implies that the mode-shaping PCF has the feature of temperature sensing. By using the simultaneous

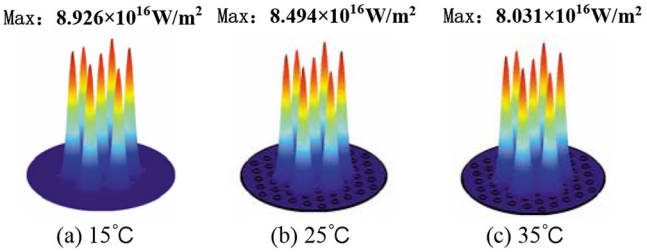

Fig. 3. Three-dimensional (3D) mode intensity distribution of the mode-shaping infiltrated PCF for different temperatures.

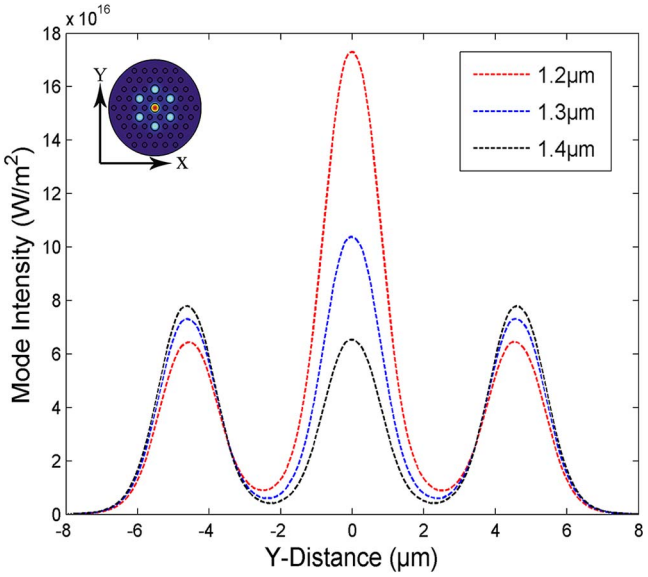

Fig. 2. Mode intensity distribution of the infiltrated cores along the y axis with diameter "a" varying from 1.2 to 1.4 μm.

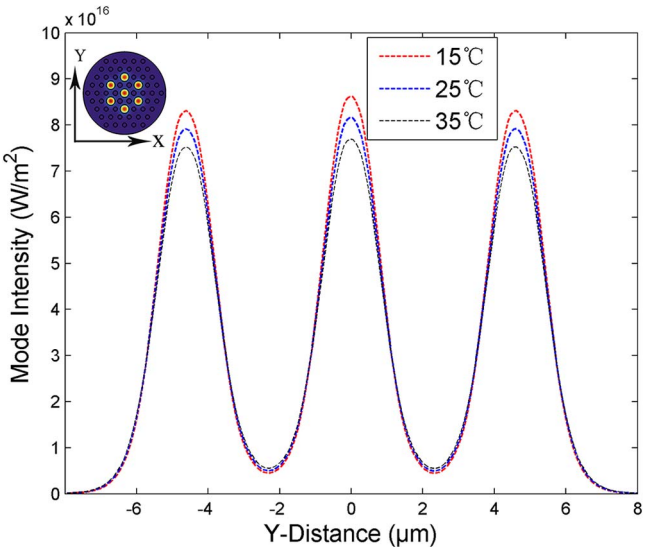

Fig. 4. Mode intensity distribution of the infiltrated cores along the y axis for different temperatures.

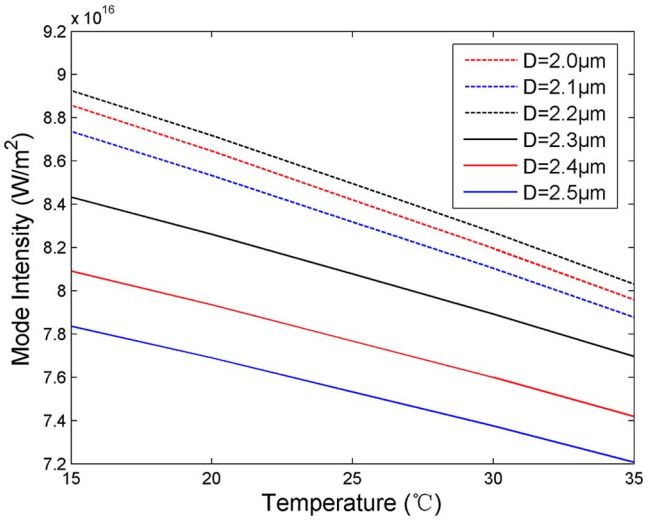

Fig. 5. Relationship between the peak value of mode intensity and the temperature at different diameters "D".

features of mode shaping and temperature sensing, it is feasible to obtain the information of the temperature by only detecting the output power of one infiltrated core with high beam quality. The sensitivity of the PCF at different diameters "D" is further shown in Fig. 6. It can be seen that the sensitivity of the PCF decreases when the diameter "D" is larger than 2.2 μm. The sensitivity can reach up to 4.475×10^{14} W/(m$^2 \cdot$ °C).

To illustrate that the mode-shaping PCF satisfies the single-mode transmission condition[22], the normalized frequency of the PCF with the same parameters of $D = 2.2$ μm, $d = 1.2$ μm, $a = 1.37$ μm, and $d/\Lambda = 0.45$ for the temperatures of 15°C, 25°C, and 35°C is shown in Fig. 7(a) with

$$V_{\mathrm{PCF}} = \frac{2\pi r}{\lambda}\sqrt{n_{\mathrm{core}}^2 - n_{\mathrm{eff}}^2}. \tag{3}$$

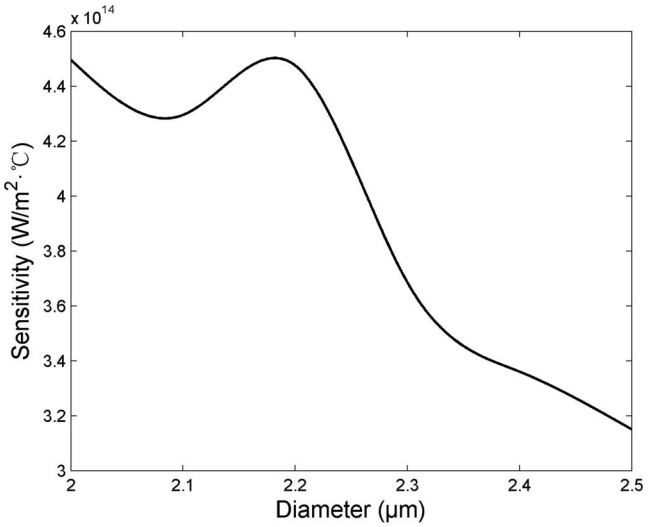

Fig. 6. Sensitivity of the PCF with different diameters "D".

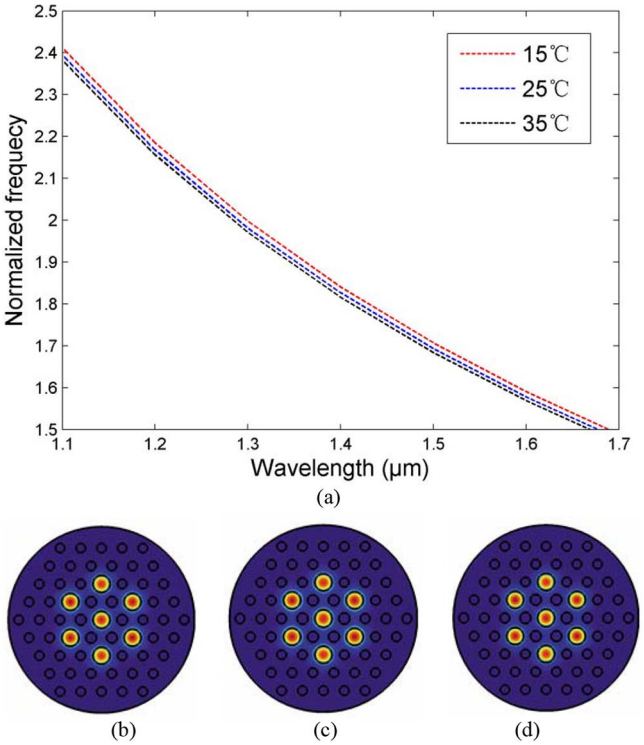

Fig. 7. (a) Normalized frequency of the infiltrated PCF for different temperatures. (b) The mode intensity with $\lambda = 1.55$ μm and $T = 15$°C. (c) The mode intensity with $\lambda = 1.55$ μm and $T = 25$°C. (d) The mode intensity with $\lambda = 1.55$ μm and $T = 35$°C.

It can be seen clearly that the normalized frequency of the PCF at the wavelength ranging from 1.1 to 1.7 μm is less than π. Hence, the infiltrated PCF supports the single-mode transmission in the communication window, which makes it suffer less from the nonlinear effects. Figures 7(b), 7(c), and 7(d) demonstrate the single-mode transmission for the temperatures of 15°C, 25°C, and 35°C, intuitively.

The effective mode field area[23] is an important parameter, which can influence the output power of the fiber and can be calculated by

$$A_{\mathrm{eff}} = \frac{(\iint |E|^2 \mathrm{d}x\mathrm{d}y)^2}{\iint |E|^4 \mathrm{d}x\mathrm{d}y}.$$

As for the mode-shaping structure with the parameters of $D = 2.2$ μm, $d = 1.2$ μm, $a = 1.37$ μm, and $d/\Lambda = 0.45$, the effective mode field area for different temperatures is shown in Fig. 8. It can be seen that the effective mode field area increases with the temperature.

It is necessary to study the waveguide dispersion of the infiltrated seven-core PCF, which can be calculated with[24]

$$D(\lambda) = -\frac{\lambda}{C}\frac{\mathrm{d}^2 \mathrm{Re}(n_{\mathrm{eff}})}{\mathrm{d}\lambda^2}. \tag{5}$$

The waveguide dispersion of the mode-shaping infiltrated PCF with $D = 2.2$ μm, $d = 1.2$ μm, $a = 1.37$ μm,

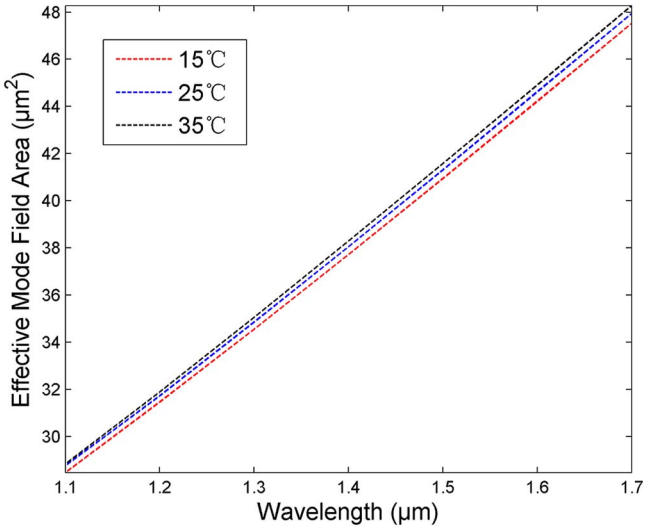

Fig. 8. Effective mode area of the infiltrated PCF for different temperatures.

and $d/\Lambda = 0.45$ is shown in Fig. 9. Once the temperature increases from 15°C to 35°C, much of the flattened waveguide dispersion can be achieved in the communication window based on the single-mode transmission.

With the mode-shaping structure of $D = 2.2$ μm, $d = 1.2$ μm, $a = 1.37$ μm, and $d/\Lambda = 0.45$, we also analyze the confinement loss, which is calculated by[25]

$$L = \frac{2\pi \times 8.686 \times \mathrm{Im}(n_{\mathrm{eff}})}{\lambda}. \tag{6}$$

The confinement loss of the infiltrated PCF for different temperatures is shown in Fig. 10. It can be observed that the designed PCF has an ultralow confinement loss although the confinement loss increases with the temperature.

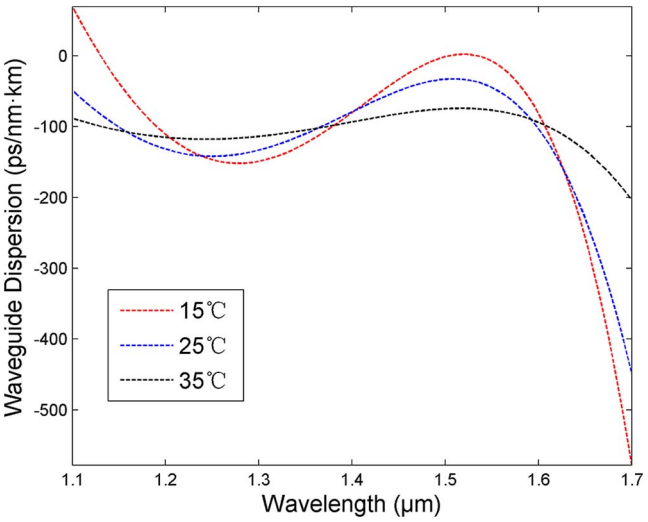

Fig. 9. Waveguide dispersion of the infiltrated PCF for different temperatures.

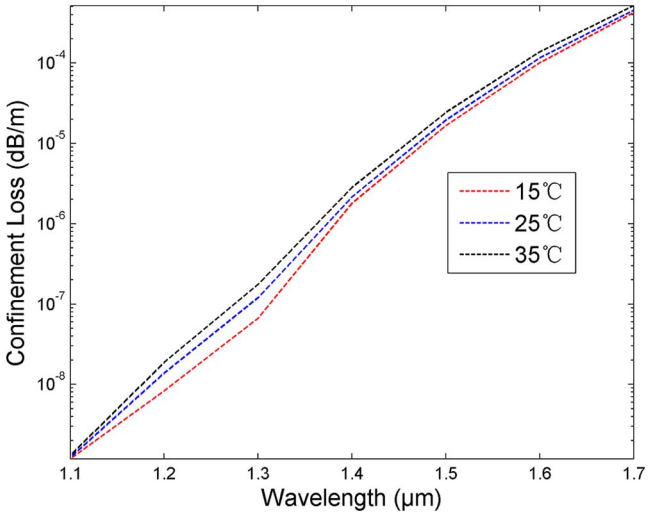

Fig. 10. Confinement loss of the infiltrated PCF for different temperatures.

We infiltrate and tailor the seven-core PCF with an E7 LC to realize simultaneous mode shaping and temperature sensing without varying the structure. Based on the mode-shaping infiltrated PCF, we observe that the mode intensity of the PCF decreases by increasing the temperature, and the peak mode intensity is inversely proportional to the temperature. However, the effective mode field area and the confinement loss increase with the temperature. A much flattened waveguide dispersion of the PCF can be implemented when the temperature is increased. The combination of mode shaping and temperature sensing allows this kind of PCF to be a good candidate for temperature sensing applications with high beam quality.

This work was supported by the Natural Science Foundation of China with under Grant No. 61475029.

References

1. P. Zu, C. C. Chan, and W. S. Lew, IEEE Photon. J. **4**, 491 (2012).
2. W. Sun, X. Liu, Q. Chai, J. Zhang, F. Fu, Y. Jiang, and T. A. Birks, Chin. Opt. Lett. **7**, 921 (2009).
3. S. K. Varshney, K. Saitoh, R. K. Sinha, and M. Koshiba, J. Lightwave Tecnol. **27**, 2062 (2009).
4. T. R. Wolinski, A. Czapla, S. Ertman, M. Tefelska, A. W. Domanski, J. Wojcik, E. Nowinowski-Kruszelnicki, and R. Dabrowski, IEEE Trans. Instrum. Meas. 57 (2008).
5. J. Zheng, Y. Yu, C. Du, P. Yan, M. Pan, J. Wang, and Z. Liu, Chin. Opt. Lett. **10**, S20611 (2012).
6. Z. Wang, Q. Li, Z. Wang, F. Zhou, Y. Bai, S. Feng, and J. Zhou, Chin. Opt. Lett. **14**, 081401 (2016).
7. J. E. Sharping, M. Fiorentino, P. Kumar, and R. S. Windeler, IEEE Photon. Technol. Lett. **14**, 77 (2002).
8. D. Noordegraaf, L. Scolari, J. Laegsgaard, L. Rindorf, and T. T. Alkeskjold, Opt. Express **15**, 7901 (2007).
9. E. Lueder, *Liquid Crystal Displays* (Wiley, 2001).
10. T. Wu and D. K. Yang, *Reflective Liquid Crystal Displays* (Wiley, 2001).
11. J. Li, C.-H. Wen, S. Gauza, R. Lu, and S.-T. Wu, IEEE/OSA J. Display Technol. **1**, 51 (2005).

12. B.-Y. Wei, P. Chen, S.-J. Ge, L.-C. Zhang, W. Hu, and Y.-Q. Lu, Photon. Res. **4**, 70 (2016).
13. B. Sun, Y. Huang, D. Luo, C. Wang, J. He, C. Liao, G. Yin, J. Zou, S. Liu, J. Zhao, and Y. Wang, IEEE Photon. J. **7**, 1 (2015).
14. T. T. Alkeskjold, J. Laegsgaard, A. Bjarklev, D. S. Hermann, J. Broeng, J. Li, S. Gauza, and S.-T. Wu, Appl. Opt. **45**, 2261 (2006).
15. H. L. Chen, S. G. Li, Z. K. Fan, G. W. An, J. S. Li, and Y. Han, IEEE Photon. J. **6**, 1 (2014).
16. N. Karasawa, Opt. Commun. **338**, 123 (2015).
17. N. Karasawa, Opt. Commun. **364**, 1 (2016).
18. S. Mathews, G. Farrell, and Y. Semenova, Microwave Opt. Technol. Lett. **53**, 539 (2011).
19. K. Milenko, T. R. Wolinski, P. P. Shum, and D. J. J. Hu, IEEE Photon. J. **4**, 1855 (2012).
20. Q. Liu, S.-G. Li, and M. Shi, Opt. Commun. **381**, 1 (2016).
21. J. Li and S.-T. Wu, J. Appl. Phys. **97**, 073501 (2005).
22. J. C. Knight, T. A. Birks, and P. J. St. Russell, Opt. Lett. **22**, 961 (1997).
23. S. Kim, C.-S. Kee, and J. Lee, J. Opt. Soc. Korea **11**, 97 (2007).
24. I. Abdelaziz, F. Abdelmalek, H. Ademgil, S. Haxha, T. Gorman, and H. Bouchriha, J. Lightwave Technol. **28**, 2810 (2010).
25. H. Ademgil and S. Haxha, IEEE J. Lightwave Technol. **26**, 441 (2008).